Electronic Supplementary Material (ESI) for CrystEngComm.

Supporting Information

Selective Synthesis of WO_3 and $W_{18}O_{49}$ Nanostructures: Ligand-free pH-Dependent Morphology Controlled Self-assembly of Hierarchical Architecture from 1D Nanostructure and Sunlight-driven Photocatalytic Degradation

Y. M. Shirke and S. Porel-Mukherjee

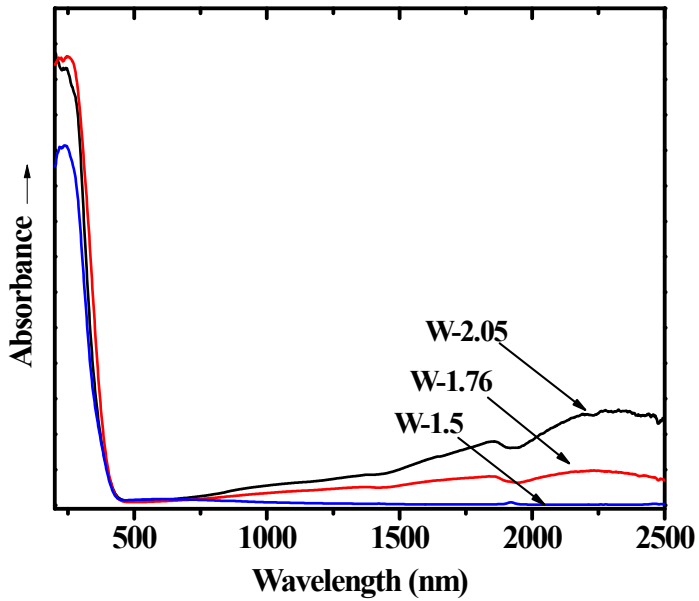

Fig. S1. UV-VIS-NIR profile comparison between products W-1.5, W-1.76 & W-2.05 and W-2.05 showing an absorption tail in the NIR region that may arise from the presence of oxygen vacancy.

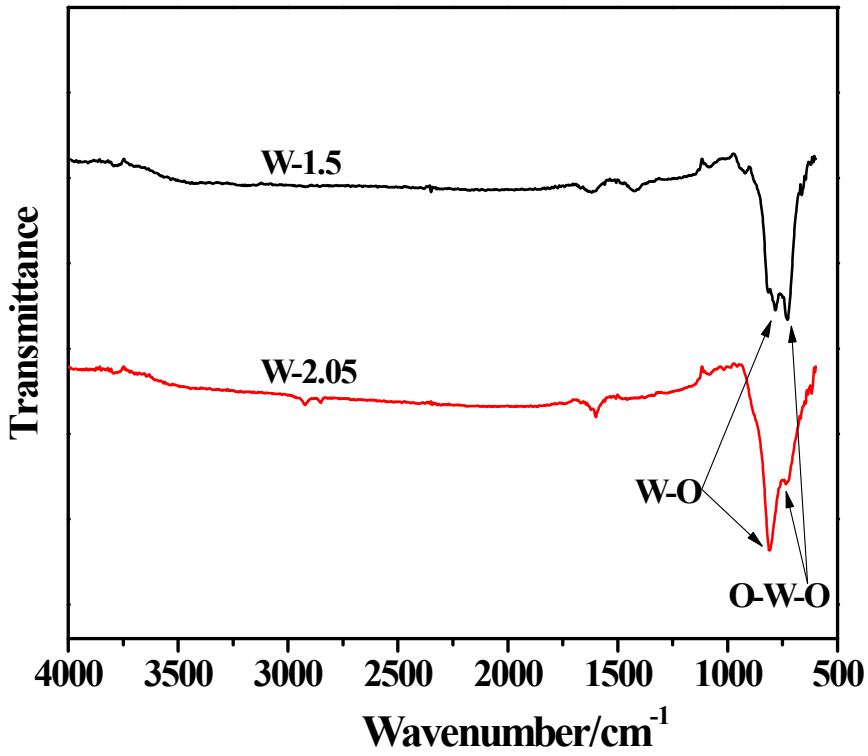

Fig. S2. FTIR spectrum of the as-prepared W-1.5 and W-2.05.

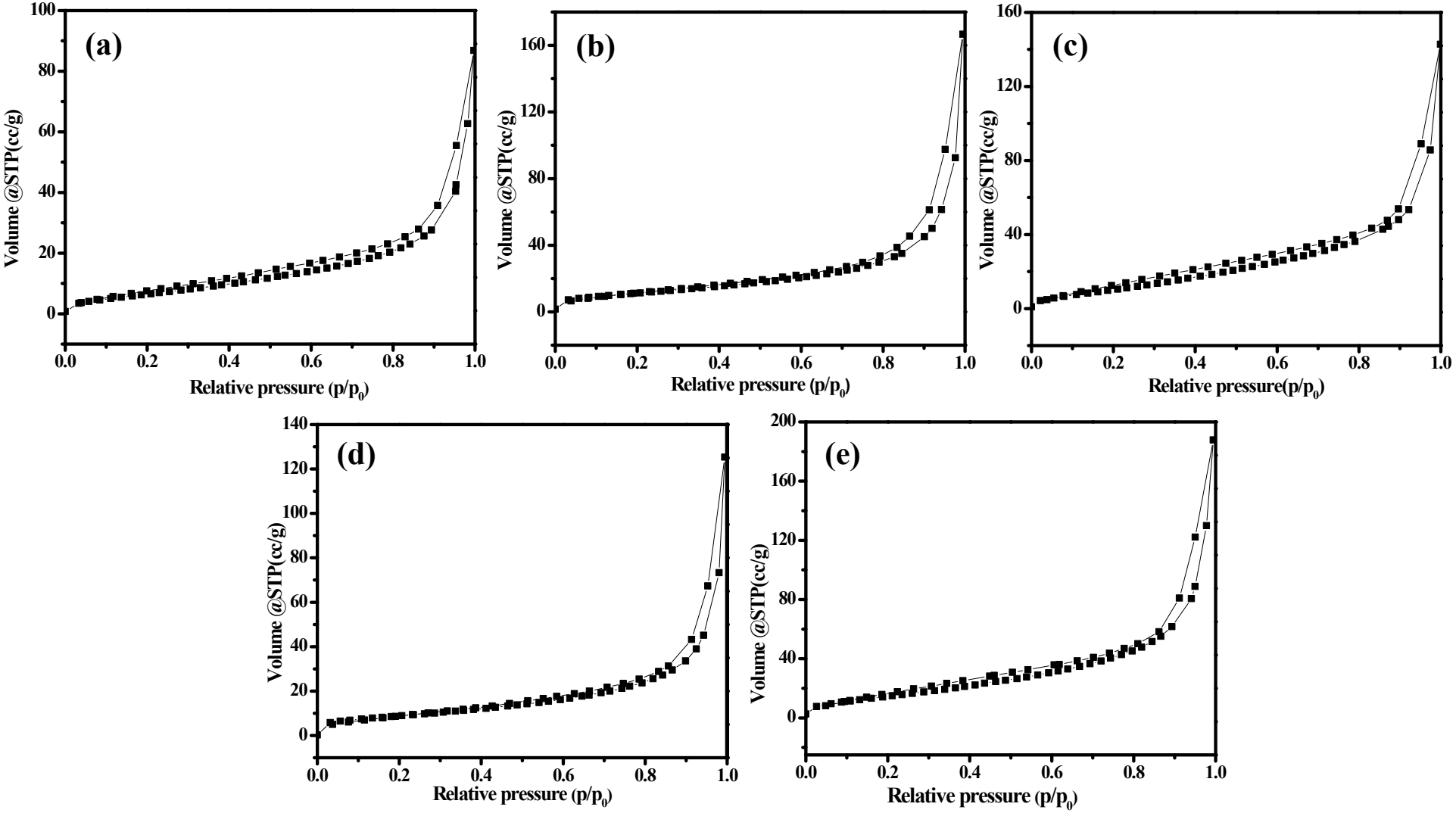

Fig. S3. N_2 adsorption/desorption isotherms for (a) W-0.95, (b) W-1.5, (c) W-1.76, (d) W-2.05 and (e) W-2.35.

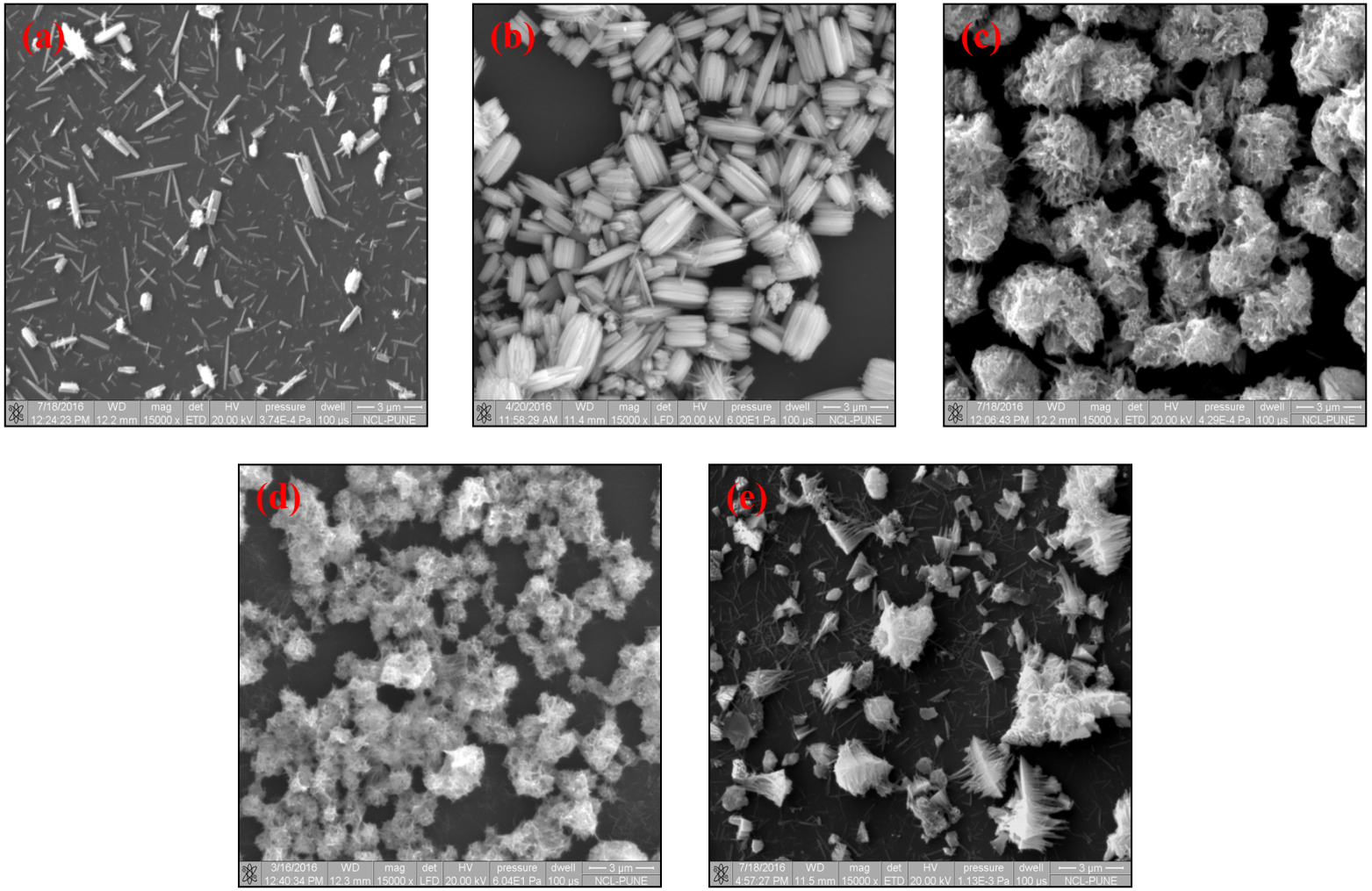

Fig. S4. SEM images of the products (a) W-0.95, (b) W-1.5, (c) W-1.76, (d) W-2.05 and (e) W-2.35. Scale bar = 3 µm

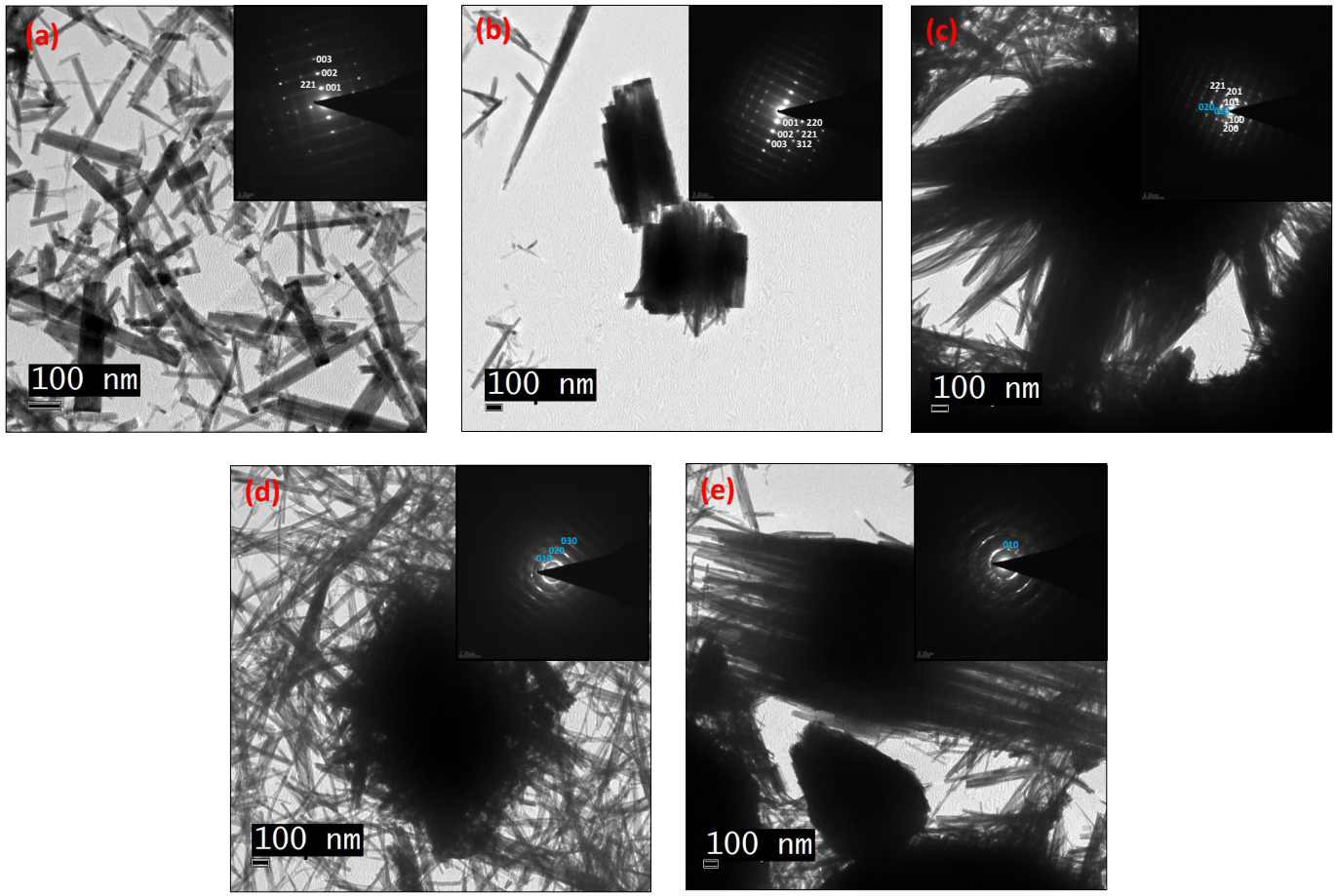

Fig. S5. TEM images and the corresponding ED pattern (inset) of the products (a) W-0.95, (b) W-1.5, (c) W-1.76, (d) W-2.05 and (e) W-2.35; with reference WO_3 (hkl = white colour) and $W_{18}O_{49}$ (hkl = blue colour).

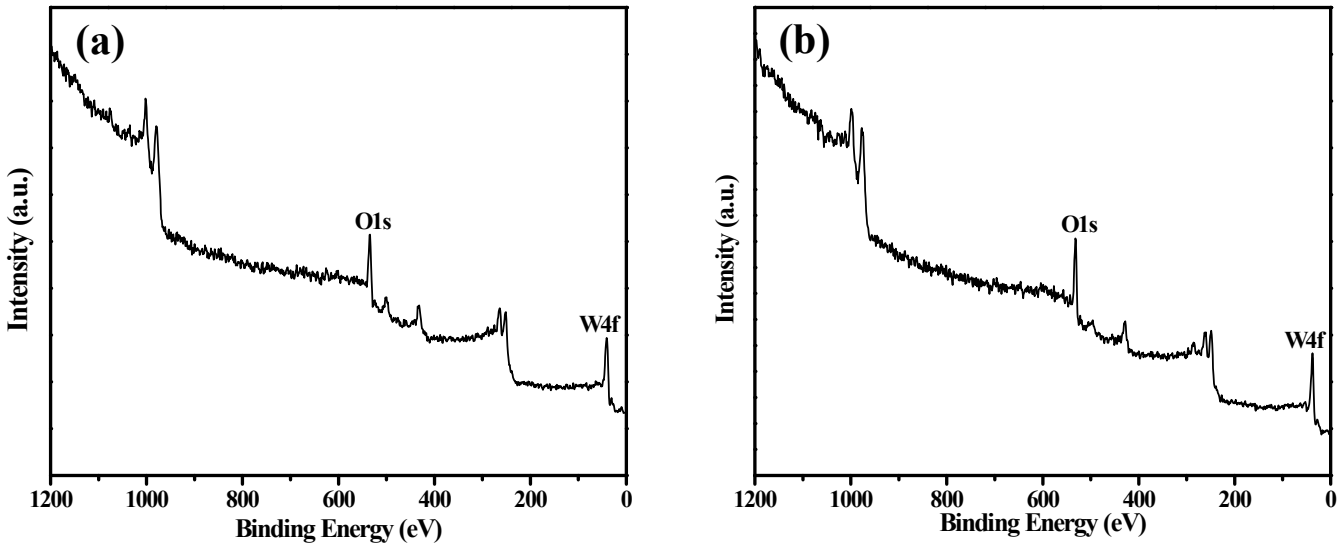

Fig. S6. Full range XPS spectra of (a) W-1.5 and (b) W-2.05

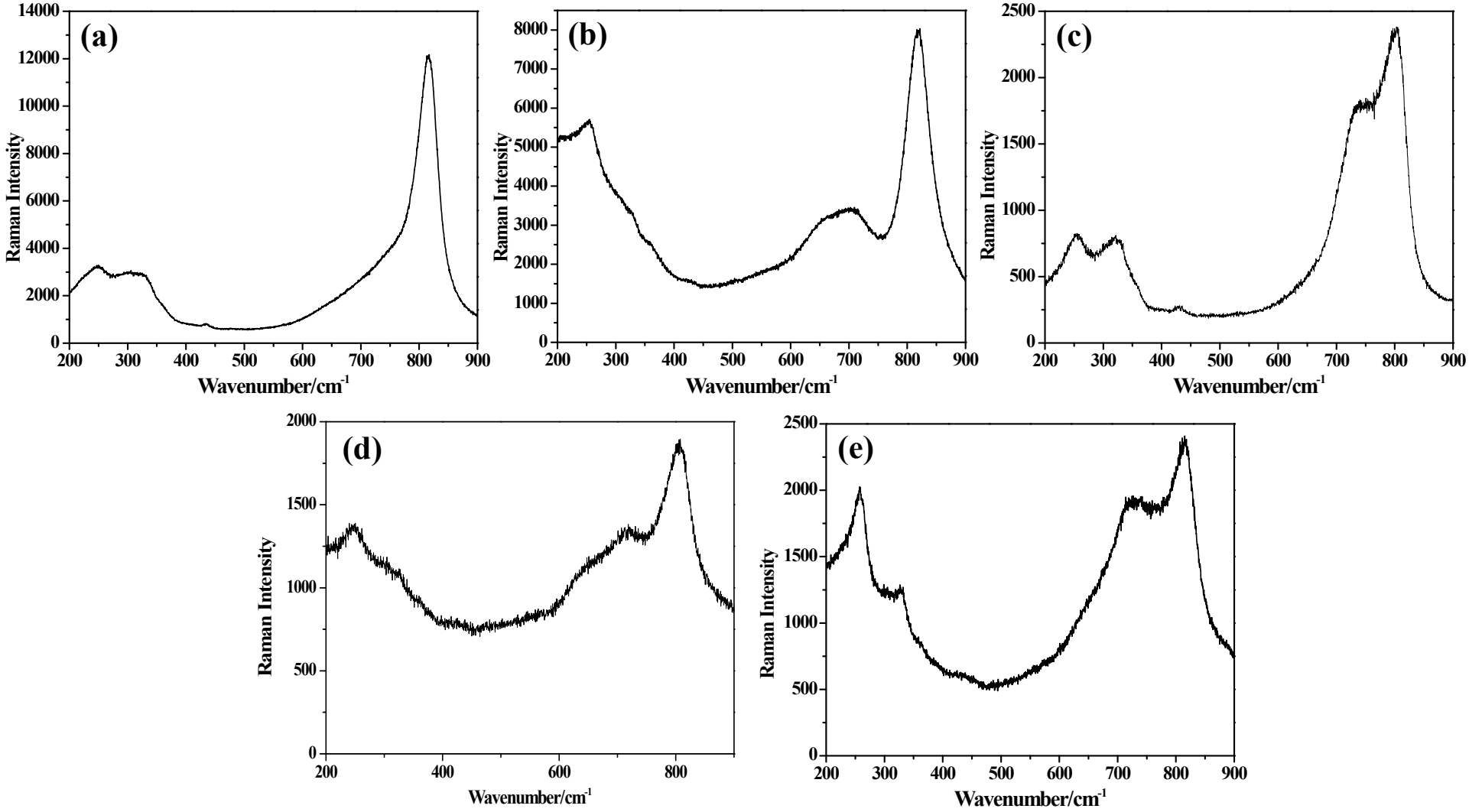

Fig. S7. Raman spectra obtained at laser power 20 mW for the products (a) W-0.95, (b) W-1.5, (c) W-1.76, (d) W-2.05 and (e) W-2.35.

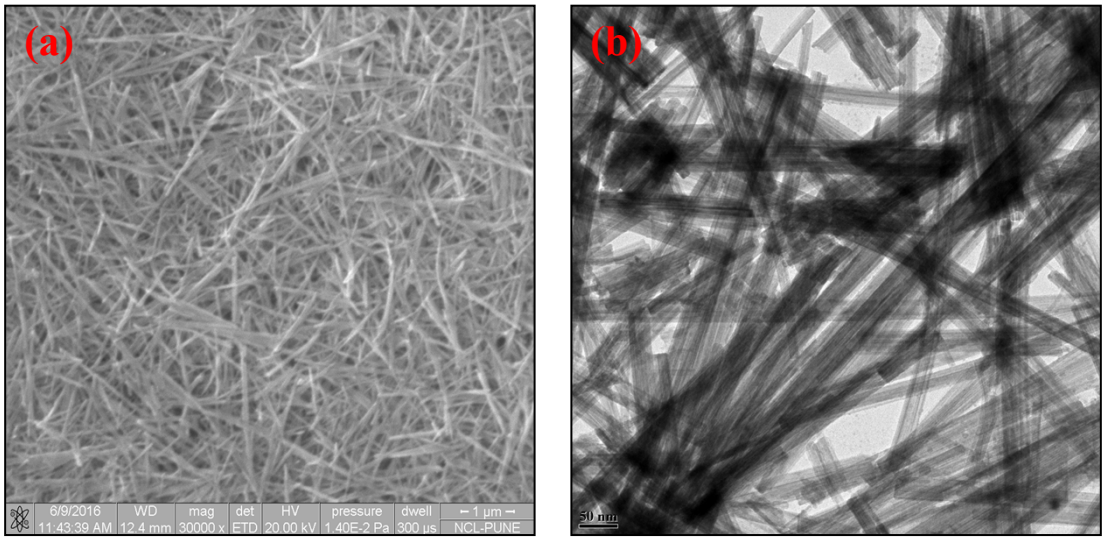

Fig. S8. (a) SEM and (b) TEM image of product W-2.35 disassembled by aqueous ultrasonication under a long treatment time.

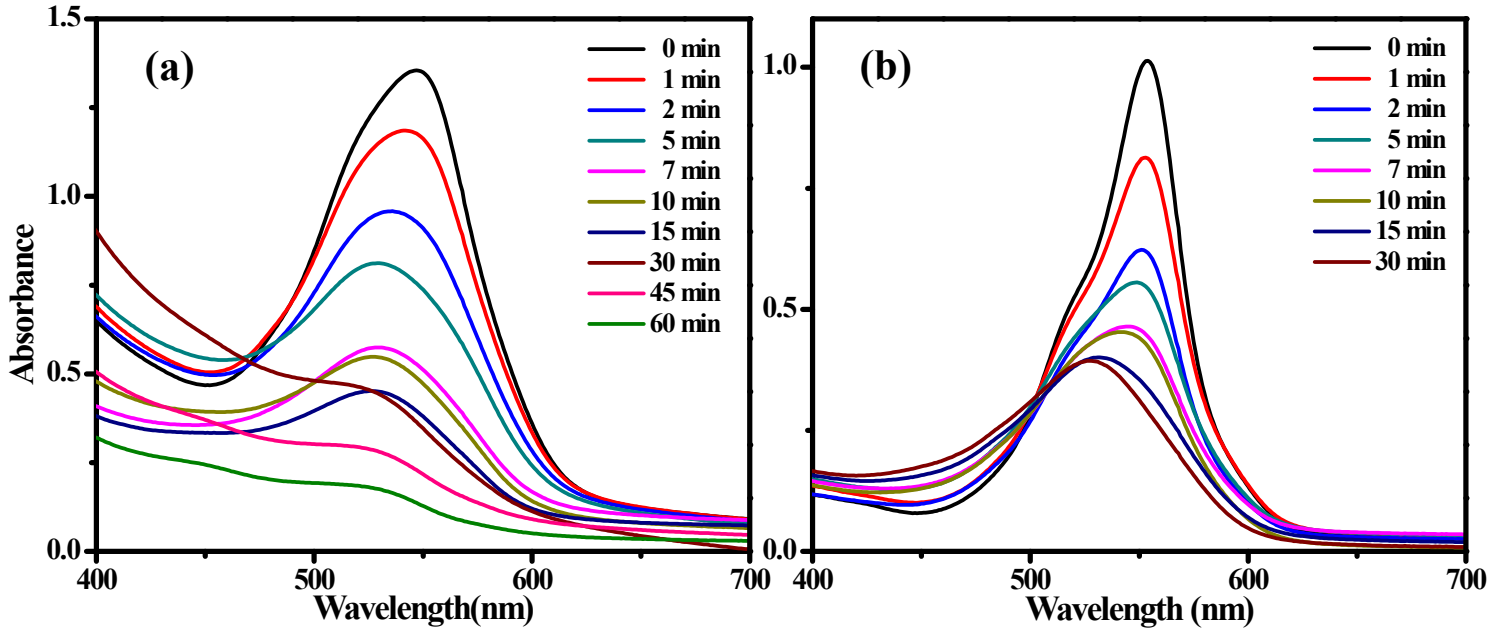

Fig. S9. The change observed in UV-Vis absorbance spectra in the presence of (a) W-1.5 and (b) W-2.05 under sunlight irradiation for different times.